Test particle simulations of resonant interactions between energetic electrons and discrete, multi-frequency artificial whistler waves in the plasmasphere*

Chang Shan-Shan(常珊珊)†, Ni Bin-Bin(倪彬彬), Zhao Zheng-Yu(赵正予), Gu Xu-Dong(顾旭东), and Zhou Chen(周 晨)

Department of Space Physics, School of Electronic Information, Wuhan University, Wuhan 430072, *China*

(Received 25 March 2014; revised manuscript received 17 April 2014; published online 20 June 2014)

Modulated high frequency (HF) heating of the ionosphere provides a feasible means of artificially generating extremely low frequency (ELF)/very low frequency (VLF) whistler waves, which can leak into the inner magnetosphere and contribute to resonant interactions with high energy electrons. Combining the ray tracing method and test particle simulations, we evaluate the effects of energetic electron resonant scattering driven by the discrete, multi-frequency artificially generated ELF/VLF waves. The simulation results indicate a stochastic behavior of electrons and a linear profile of pitch angle and kinetic energy variations averaged over all test electrons. These features are similar to those associated with single-frequency waves. The computed local diffusion coefficients show that, although the momentum diffusion of relativistic electrons due to artificial ELF/VLF whistlers with a nominal amplitude of ~ 1 pT is minor, the pitch angle scattering can be notably efficient at low pitch angles near the loss cone, which supports the feasibility of artificial triggering of multi-frequency ELF/VLF whistler waves for the removal of high energy electrons from the magnetosphere. We also investigate the dependences of diffusion coefficients on the frequency interval (Δf) of the discrete, multi-frequency waves. We find that there is a threshold value of Δf for which the net diffusion coefficient of multi-frequency whistlers is inversely proportional to Δf (proportional to the frequency components $N_{\rm w}$) when Δf is below the threshold value but it remains unchanged with increasing Δf when Δf is larger than the threshold value. This is explained as being due to the fact that the resonant scattering effect of broadband waves is the sum of the effects of each frequency in the 'effective frequency band'. Our results suggest that the modulation frequency of HF heating of the ionosphere can be appropriately selected with reasonable frequency intervals so that better performance of controlled precipitation of high energy electrons in the plasmasphere by artificial ELF/VLF whistler waves can be achieved.

Keywords: wave–particle interactions, test particle simulations, discrete multi-frequency whistler waves, ionospheric modification

PACS: 94.20.wj, 94.30.Ny, 94.20.Vv, 94.30.Tz **DOI:** 10.1088/1674-1056/23/8/089401

1. Introduction

There has been increasing concern regarding the dynamics of energetic radiation belt electrons over the past decades, and various simulation models of radiation belt electron dynamics have been developed.[1–7] In the basically collisionless magnetosphere, changes in energetic electron population are significantly controlled by resonant interactions with a variety of naturally forming plasma waves,[8–17] such as whistler-mode chorus, plasmaspheric hiss, electromagnetic ion cyclotron (EMIC) waves, etc. An additional potential mechanism has also been proposed and studied,[18–24] by using artificial extremely low frequency (ELF)/very low frequency (VLF) waves generated by ground-based or satellite-based transmitters or by modulated high frequency (HF) heating of the ionosphere, to actively control/modify the energetic electron lifetimes and consequently the energetic electron population. While many studies followed the quasi-linear theory to evaluate the electron diffusion effects of these artificial ELF/VLF waves,[18,19,21–23] test particle simulations were also implemented by Inan *et al*. that only considered the wave propagation along the magnetic field lines to assess the electron precipitation caused by ground-based VLF transmitters,[20] and by Chang *et al*. that combined the ray tracing and test particle simulations to investigate the local resonant diffusion of the energetic electrons induced by highly oblique monochromatic (single-frequency) ELF/VLF waves due to ionosphere modification.[24]

In the present study we follow the method presented by Chang *et al*.[24] but perform a detailed investigation on the electron scattering effects of discrete, multi-frequency artificial whistlers, since it has been practically feasible to run HF heating experiments to trigger artificial ELF/VLF waves at a number of frequencies[21–24] and produce a broadband frequency spectrum in a certain spatial region. Considering that these broadband artificial waves are discrete and the frequency interval is an important quantity, we evaluate the dependences

*Project supported by the National Natural Science Foundation of China (Grant Nos. 41204120 and 41304130) and the Fundamental Research Funds for the Central Universities (Grant No. 2042014kf0251).

†Corresponding author. E-mail: whu.css1108@gmail.com

© 2014 Chinese Physical Society and IOP Publishing Ltd

of the diffusion coefficients on the frequency intervals of the artificial broadband waves.

The remainder of this study is organized as follows. In Section 2 we present our ray tracing results of ELF/VLF emissions at frequencies of our interest. In Section 3, the resonance conditions between artificial ELF/VLF waves and energetic electrons in the plasmasphere are investigated to identify the energy and pitch angle of electrons in resonance with the artificially generated ELF/VLF whistlers. The test particle model and the simulation results are presented in Section 4. The temporal variations of multiple electron energy and pitch angle, due to resonant interactions with discrete, multi-frequency waves, are clarified and used to evaluate the average effect of wave-induced localized pitch angle scattering and momentum diffusion. The dependence of local diffusion coefficient on the adoption of frequency interval is also analyzed. In Section 5 we summarize our conclusions, and also discuss our results and the limitations of this study for future improvement.

2. Ray tracing simulations of whistler-mode waves generated by modulated ionospheric heating

The generation of electromagnetic waves in the ELF and VLF bands by modulated HF heating of the ionospheric current system has been investigated experimentally.[25–28] There have been a number of observations indicating that some of these artificial ELF/VLF waves can propagate directly upwards and penetrate through the ionosphere into the magnetosphere, and others propagate within the earth–ionosphere waveguide and leak up progressively.[25,26] The wave intensity detected by a ground-based receiver or by a spacecraft instrument is generally at a magnitude of a few picoteslas.[25–28] Since there have been a number of ionospheric heating attempts at low latitudes such as Arecibo besides those at higher latitudes such as HAARP, the present study is directed towards exploring the artificial triggering of ELF/VLF waves at low latitudes. During the Arecibo experiments, ELF/VLF waves were produced over a frequency range from 500 Hz to 5 kHz using a heater frequency of approximately 3 MHz and a total HF input power of 800 kW.[28] Thus we concentrate on the artificially triggered waves at 800 Hz–1000 Hz, which are much lower than the range of 17 kHz–23 kHz investigated by Abel and Thorne and represent the particular interest of the present study.

We have developed a cold plasma ray-tracing model to simulate the propagation of these ELF waves from the ionospheric generation region upward into the magnetosphere, excluding the damping/growth of the waves. The magnetosphere is an inhomogeneous magnetoplasma, and the wave energy, in general, propagates in a direction different from the wave normal angle, referred to as the ray direction.[29,30] The ray tracing equations, which are a set of first order differential equations, describe the variations of the ray position and wave normal vector with time.[24,29,30] By solving the ray tracing equations with a proper setting of initial values and a background model description of the magnetosphere, the entire trajectory of the wave energy (i.e. the ray path) and the wave normal angle can be determined. Here we focus on the spatial region confined to $L < 6$, for which we choose a dipole field and the cold plasma diffusion equilibrium model.[24,29,30] Readers are referred to the paper by Chang *et al*.[24] and references therein for more details of the adopted ray tracing model.

To initiate the ray tracing simulations, we select three frequencies, i.e. 800, 900, and 1000 Hz, and assume that these ELF waves are already triggered by modulating the ionospheric currents and launched at an altitude of 120 km and magnetic latitude of 15°. In addition, the initial angle between the wave normal and the radial vector is set to be 0° for all cases considered below.

According to the ray tracing results shown in Figs. 1(a)–1(c) for the three specific wave frequencies, these artificial whistler waves, once leaking into the magnetosphere from the lower ionosphere, can reflect between the southern and northern hemispheres, propagate outwards, and finally settle down at certain L shells. Apparently, the ray path varies strongly with wave frequency; that is, lower frequency waves can propagate outwards to farther distances, thus reaching higher L shells with a broader spatial coverage. Specifically, the 800 Hz wave can reach $L = 3.2$, the 900 Hz wave settles down at about $L = 3.1$, and the 1000 Hz wave tends to become stable at $L = 3$. This implies that ELF waves at 800 Hz–1000 Hz, once triggered by modulated HF heating of the ionosphere, should all reach the region of $L = 3$ and contribute to wave–particle interactions there.

Figure 1(d) shows the temporal variation of wave normal angle indicated as the bold curve (labeled left) and of latitude as the fine curve (labeled right) for 1000 Hz waves (corresponding to Fig. 1(c)). The wave normal angle changes around 90° (each magnetospheric reflection occurs when ψ is 90°) and eventually tends to stabilize at 90°. It is evident that these artificial ELF waves are highly oblique when propagating in the magnetosphere. Actually, the waves have become quasi-resonant waves when they are stabilized at a certain L shell and the magnetospheric reflection occurs more easily. As indicated in Fig. 1, many more reflections occur in a region $L = 2$–3 than $L < 2$. This can be related to the lower hybrid resonance (LHR), which can significantly influence the wave propagation when the wave normal angle is close to 90°, corresponding to the so-called quasi-resonance regime of propagation.[31] Moreover, since the quasi-resonance regime of propagation is sensitive to the LHR frequency profile, the background plasma parameters largely determine the LHR frequency and consequently strongly affect the stable point.

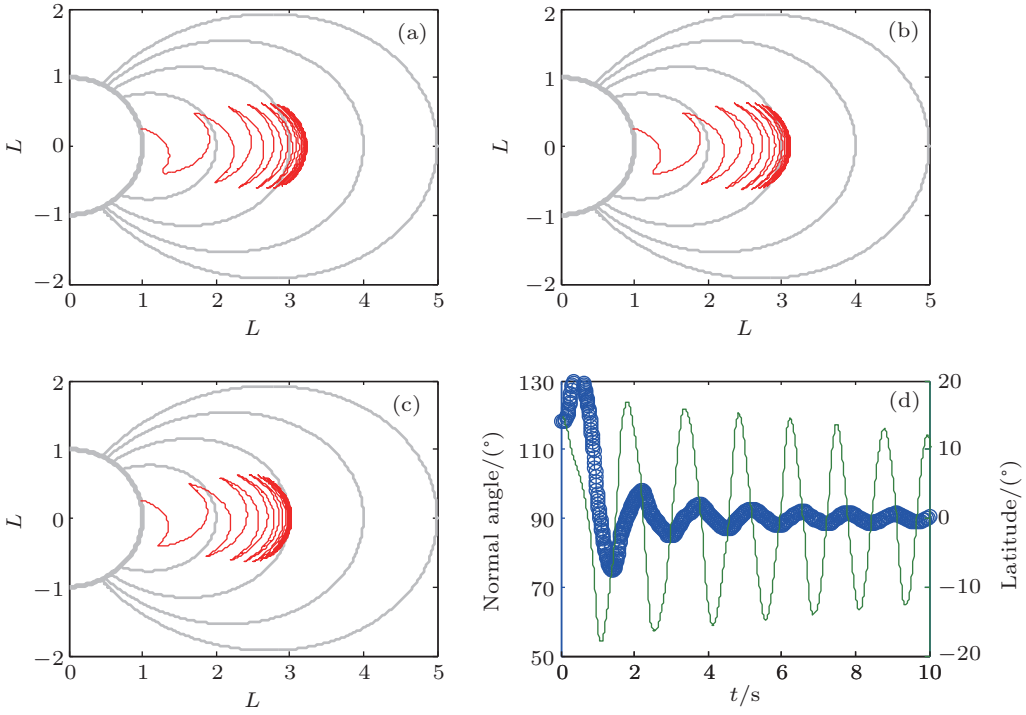


Fig. 1. (color online) Ray tracing results of artificially triggered whistler waves at different frequencies: (a) $f = 800$ Hz, (b) $f = 900$ Hz, (c) $f = 1000$ Hz, and (d) the temporal variation of wave normal angle and latitude for the 1000 Hz wave corresponding to (c).

After these ELF whistler-mode waves, artificially generated by ionospheric modification, leak into the magnetosphere for propagation, they encounter a highly active particle environment, thus providing a potential for resonant interactions with energetic electrons in the plasmasphere, which will be investigated in detail in the following sections.

3. Wave–particle resonant interaction condition

When we have the information about the wave property, the background magnetic field, and electron density, we can evaluate electron energies in resonance with the indicated broadband waves at a fixed location in the magnetosphere, following the relativistic resonance condition

$$\omega - \mathrm{k}_{\|} v_{\|} = \frac{N|\Omega_{\mathrm{e}}|}{\gamma} = 0, \pm 1, \pm 2, \ldots, \tag{1}$$

where ω is the wave frequency; $k_{\|} = k\cos\psi$ is the wave number component parallel to the ambient magnetic field with $k = \mu\omega/c$ being the total wave number and ψ being the wave normal angle, μ being the phase refractive index, calculated using the cold plasma theory; $v_{\|} = v\cos\alpha$ is the particle velocity component parallel to the ambient magnetic field with α being the pitch angle; N is the resonance harmonic number; Ω_{e} is the electron gyrofrequency; γ is the Lorentz factor given by $\gamma = (1-\beta^2)^{-1/2}$ with $\beta = v/c$. As seen from Eq. (1), after the wave frequency, the wave normal angle, the ambient density, the magnetic field, and the resonance harmonic are specified, the energy of the particles can be obtained for any value of α.

Figure 2 shows the energies of electrons that resonate with the artificial ELF/VLF waves at 800 Hz–1000 Hz as a function of pitch angle for the resonance harmonic $N = 1$ at the equator of $L = 3$. This location is within the spatial coverage of the 800 Hz–1000 Hz wave propagation (Figs. 1(a)–1(c)). According to Fig. 1(d), the wave normal angle is set to be 95° at the equator. Apparently, only resonances with positive harmonic numbers, e.g. $N = 1, 2, 3$, can occur. Note that we have assumed that the electrons move in the positive direction with respect to the z axis.

As shown in Fig. 2, regarding the energy and pitch angle (α, E) of the electrons that can undergo resonances with these artificially triggered whistler waves at 800 Hz–1000 Hz, there are a number of interesting features to note. (i) Electrons with (α, E)-values within the marked grey area satisfy the first-order ($N = 1$) resonance condition with the 800–1000 Hz waves and potentially interact with them. The triggered waves can resonate with electrons from $\sim$ 600 keV to $\sim$ 10 MeV. (ii) For a fixed electron energy, such as 700 keV, 1 MeV or 2 MeV marked by the horizontal dotted lines, there is a certain pitch angle range within which electrons can resonate with the 800 Hz–1000 Hz waves. Specifically, the pitch angle range is 0°–28° for 700 keV electrons, 37°–48° for 1 MeV electrons, and 64°–68° for 2 MeV electrons. (iii) The resonant energy increases with increasing pitch angle. They also show a sharp gradient for pitch angles from 60° to 90°, which is mainly due

to quickly reduced $v_{\parallel}$ in the resonance condition. We note that for other resonance harmonics the areas of (α, E) in resonance should be different, and can either absolutely differ from or partially intersect with that for $N = 1$. For the case considered here, i.e. 800 Hz–1000 Hz whistler waves at the equatorial $L = 3$, the resonant energy for $N = 2$ (not shown) is much higher than that for $N = 1$ and there is no overlap, indicating that electrons with the energy and pitch angle (α, E) within the marked grey area in Fig. 2 can only resonate with the artificial waves under the first-order resonance harmonic.

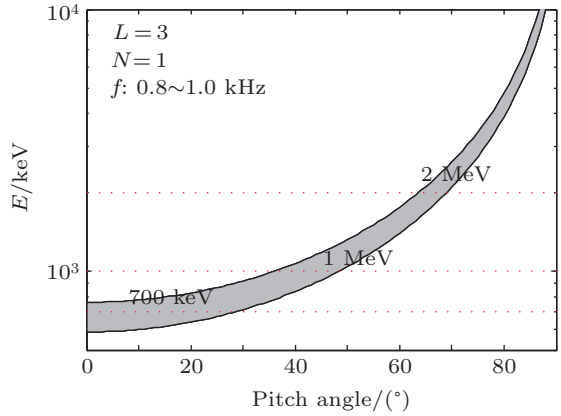


Fig. 2. Electron resonant energies as a function of pitch angle corresponding to the interaction with the artificially generated whistler waves at frequencies of 800–1000 Hz for the resonance harmonic $N = 1$ at the equatorial region of $L = 3$.

4. Test particle simulations

4.1. Particle motion equations

To perform test particle simulations, we follow Chang *et al.*[24] to use the following relativistic Lorentz equation:

$$\frac{\mathrm{d}\boldsymbol{x}}{\mathrm{d}t} = \frac{\boldsymbol{p}}{\gamma m}, \tag{2a}$$

$$\frac{\mathrm{d}\boldsymbol{p}}{\mathrm{d}t} = q\left[\boldsymbol{E}_{\mathrm{w}} + \frac{\boldsymbol{p}}{\gamma m} \times (\boldsymbol{B}_{\mathrm{w}} + \boldsymbol{B}_{\boldsymbol{0}})\right], \tag{2b}$$

where $\boldsymbol{p}$ is the electron momentum, and m and q are the rest mass and charge of an electron respectively. For simplicity, we use a homogeneous background magnetic field $\boldsymbol{B}_0 = B_0\boldsymbol{e}_{\boldsymbol{z}}$ in our simulation[24,32] as we focus on the resonance effect of local (around the magnetic equator) artificial ELF/VLF waves. The discussion of this simple assumption is deferred to Section 5. Since we study the effect of artificially generated multi-frequency whistlers, different from the single-frequency wave as studied by Chang *et al.*,[24] the net magnetic and electric fields of the artificial whistler ELF waves with the multiple wave normal vectors $\boldsymbol{k}_j = k_j(\sin\psi_j, 0, \cos\psi_j)$ are given by

$$\boldsymbol{B}_{\boldsymbol{w}} = \sum_{\mathrm{j}=1}^{N_{\mathrm{w}}} (B_{xj}^{\mathrm{w}}\cos\Phi_j\boldsymbol{e}_{\boldsymbol{x}} - B_{yj}^{\mathrm{w}}\sin\Phi_j\boldsymbol{e}_{\boldsymbol{y}} + B_{zj}^{\mathrm{w}}\cos\Phi_j\boldsymbol{e}_{\boldsymbol{z}}), \tag{3a}$$

$$\boldsymbol{E}_{\boldsymbol{w}} = \sum_{j=1}^{N_{\mathrm{w}}} (-E_{xj}^{\mathrm{w}}\sin\Phi_j\boldsymbol{e}_{\boldsymbol{x}} - E_{yj}^{\mathrm{w}}\cos\Phi_j\boldsymbol{e}_{\boldsymbol{y}} - E_{zj}^{\mathrm{w}}\sin\Phi_j\boldsymbol{e}_{\boldsymbol{z}}), \tag{3b}$$

where $\boldsymbol{e}_z$ is along the direction of background magnetic field, and $\boldsymbol{e}_x$ and $\boldsymbol{e}_y$ are the unit vectors within the equatorial plane, completing the right-hand coordinate system. The wave amplitudes B_{xj}^{w}, B_{zj}^{w}, E_{xj}^{w}, E_{yj}^{w}, E_{zj}^{w} of the jth frequency component $f_j = f_{\min} + j\Delta f, j = 1, 2, \ldots, N_{\mathrm{w}}$, can be calculated by a chosen B_{yj}^{w}.[24,33,34] The wave phase angle of each frequency component is $\Phi_j = k_j z - \omega_j t + \phi_{0j}$, with the initial wave phase angle ϕ_{0j} randomly chosen between 0 and 2π and wave number k_j calculated using the cold plasma theory.

4.2. Simulation parameters

Here we select the location of $L = 3$ and the wave normal angle to be 95°, according to the ray tracing results. f_j is set to be within 800 Hz–1000 Hz with $f_{\min} = 800$ Hz and the total bandwidth $N_{\mathrm{w}}\Delta f = 200$ Hz. Consequently, $f_{\max} = 1000$ Hz. Note that the interval between frequencies Δf is an essential quantity in the simulation of test particles, which will be shown below. In the present study Δf is chosen to be 0.1, 0.2, 0.5, and 1 Hz. Correspondingly, the total numbers of generated frequencies are 2000, 1000, 400, and 200. By doing so, we aim to investigate the effects of various triggering patterns of multi-frequency artificial whistlers on scattering energetic electrons in the plasmasphere. According to the previous *in-situ* observations of ELF/VLF whistler waves generated by HF heating facilities, B_{yj}^{w} is nominally taken to be 1 pT for all wave components at different frequencies.

We focus on tracing the temporal variations of electron pitch angle and kinetic energy driven by HF heating triggered local waves at frequencies in a range of 800 Hz–1000 Hz. We use an ensemble of 100 electrons that have identical values of initial pitch angle and energy (α, E) but have random initial gyro-phases (the angle between $\boldsymbol{v}_{\perp}$ and $\boldsymbol{e}_{\boldsymbol{x}}$) and z coordinates to evaluate wave-induced average change of (α, E) and quantify the corresponding rates of pitch angle scattering and energy diffusion.

Before discussing our simulation results in detail, we point out that all test particle simulation results presented are local values, namely, at one point in space. Strictly, inclusion of the background magnetic field topology and a bounce-averaged procedure is appropriate to apply 'long term' averaging over particle bounce orbits and obtain more representative features. However, in this study we intend to concentrate on electron scattering effects locally induced by discrete, multi-frequency artificial waves and their underlying dependence on frequency interval (in other words, the number of frequencies) of artificially generated whistlers. While test particle exploration of the wave scattering effect in an inhomogeneous, more realistic magnetic field model is beyond the scope of the present investigation, we defer the discussion on the limitation of our local diffusion computations to Section 5.

4.3. Results

We first present the cases of electrons with a pitch angle of 10° and an energy of 700 keV. We investigate in detail the pitch angle scattering and momentum diffusion driven by artificial broadband whistler waves ranging from 800 Hz to 1000 Hz with four different frequency intervals, i.e., $\Delta f = 0.1$, 0.2, 0.5, and 1 Hz. The corresponding numbers of considered wave frequencies are 2001, 1001, 401, and 201, respectively. As shown in Fig. 2, theoretically, 700 keV electrons with 10° pitch angle can resonate with the 800 Hz–1000 Hz artificial waves under the first order resonance harmonic.

The test particle simulation results are shown in Fig. 3. The top two rows show the wave-induced temporal changes of pitch angle and kinetic energy of five test electrons randomly chosen from the total population of 100 electrons. On the one hand, the behavior of each electron is apparently stochastic over the 200 gyroperiods for the four adopted frequency interval cases. The stochastic behavior of test electrons results from the fact that the distance between two adjacent resonances is smaller than the sum of the halfwidths of the two resonance islands.[32] On the other hand, the frequency interval tends to strongly affect the magnitudes of changes in pitch angle and energy of electrons. Specifically, the wave induced changes in pitch angle and energy are generally largest for $\Delta f = 0.1$ Hz, varying between $\pm 0.2°$ for pitch angle and ± 0.03 keV for energy, respectively. These variations decrease as the frequency interval increases to 1 Hz. The two bottom rows show the magnitudes of $\Delta\alpha^2$ ($\Delta\alpha = \alpha - \alpha_0$) and ΔE^2 ($\Delta E = E - E_0$) averaged over all 100 test electrons. Interestingly, $\langle \Delta\alpha^2 \rangle$ or $\langle \Delta E^2 \rangle$ increases nearly monotonically with time and demonstrates an almost linear profile. These features are similar to those associated with electron interactions with single-frequency waves.[24]

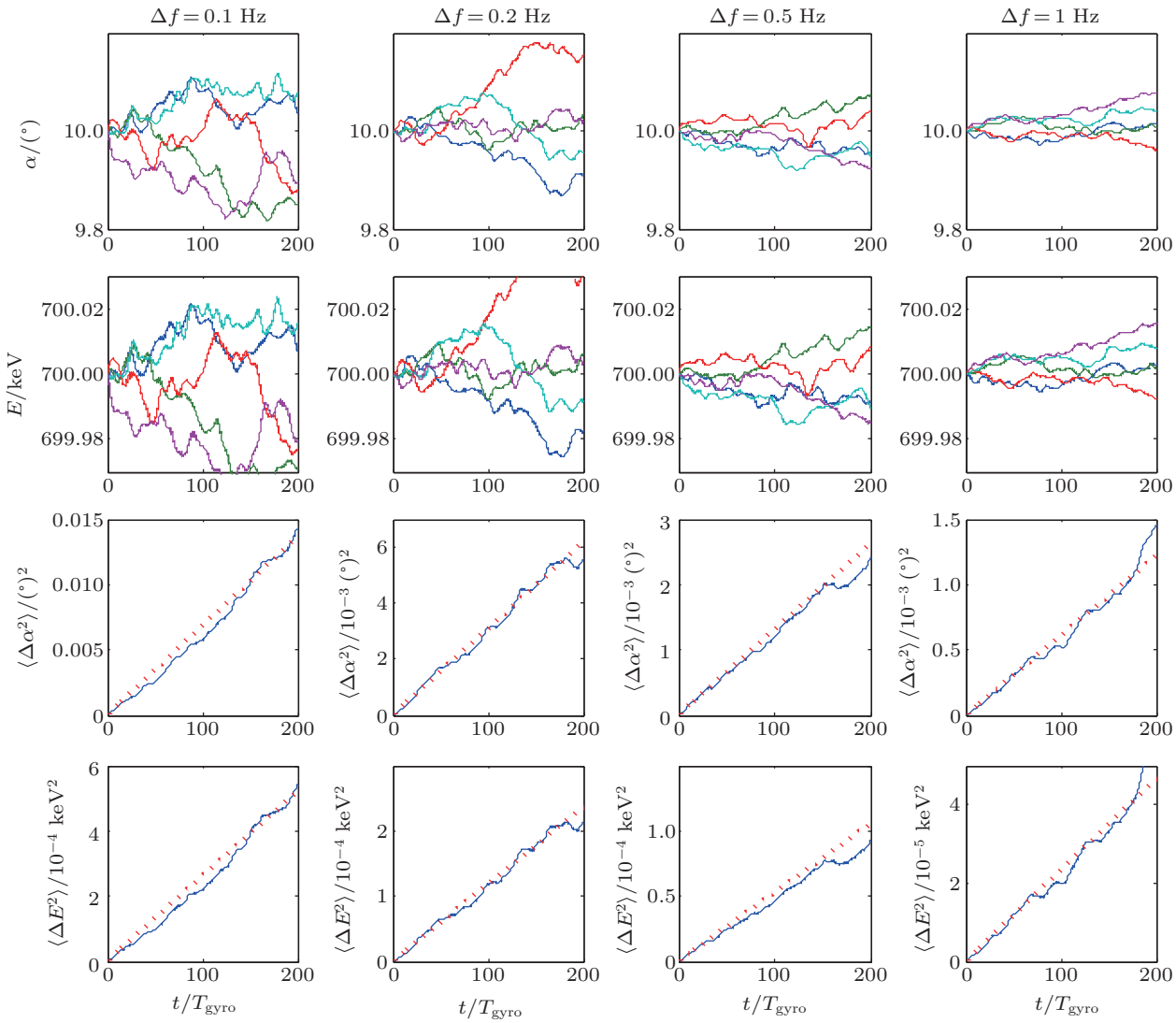


Fig. 3. (color online) Results of pitch angle scattering and momentum diffusion of electrons with an initial energy of 700 keV and an initial pitch angle of 10° due to resonant interactions with the 800–1000 Hz artificial whistler waves, for four indicated frequency intervals, i.e., $\Delta f =$ 0.1, 0.2, 0.5, and 1 Hz.

It is necessary and straightforward to present our test particle scattering results in the form of diffusion coefficients,[35–37] which are calculated as

$$D_{\alpha\alpha}^{\mathrm{TP}} = \langle \Delta\alpha^2 \rangle / 2\Delta t, \tag{4a}$$

$$D_{EE}^{\mathrm{TP}} = \langle \Delta E^2 \rangle / 2\Delta t. \tag{4b}$$

Furthermore, test particle diffusion coefficients are obtained by applying fitting as $y = A + Bt$ to the temporal curves $\Delta\alpha^2$ and ΔE^2 with $D_{\alpha\alpha}^{\mathrm{TP}}(D_{EE}^{\mathrm{TP}}) = B/2$,[32] of which the results are indicated by the dotted curves in the two bottom rows. Note that $|A|$ is close to zero, and much smaller than B for all cases in Fig. 3. The computed values of localized pitch angle diffusion coefficient ($D_{\alpha\alpha}^{\mathrm{TP}}$) are 1.35×10^{-4}, 6.27×10^{-5}, 2.46×10^{-5}, and 1.25×10^{-5} rad^2 s^{-1}, and the computed values of localized momentum diffusion rate (D_{EE}^{TP}) are 1.61×10^{-8}, 7.86×10^{-9}, 3.09×10^{-9}, and 1.56×10^{-9} MeV^2 s^{-1}, for $\Delta f = 0.1$, 0.2, 0.5, and 1 Hz, respectively. These results show that $D_{\alpha\alpha}^{\mathrm{TP}}$ (D_{EE}^{TP}) is approximately inversely proportional to Δf. This can be explained as being due to the corresponding changes in total wave power with variation of frequency number, since quasi-linear diffusion coefficients scale linearly with the total wave power, which is calculated as $\sim N_{\mathrm{w}}(B_{yj}^{\mathrm{w}})^2$ for discrete, multi-frequency waves[32] with $N_{\mathrm{w}}\Delta f \equiv 200$ Hz and $B_{yj}^{\mathrm{w}} \equiv 1$ pT for the present study.

Figure 4 shows similar results but for electrons with a pitch angle of 45° and an energy of 1 MeV. It is clearly demonstrated that an electron diffusion process occurs due to resonant interactions with the 800–1000 Hz whistler waves triggered by HF ionospheric heating. As shown in Fig. 3, the wave-induced changes in pitch angle and energy of each test electron are stochastic, while the averaged effect shows temporal linearity. Obviously, the computed $D_{\alpha\alpha}^{\mathrm{TP}}$ and D_{EE}^{TP} are also inversely proportional to Δf. While the total wave power is the same, we note that the pitch angle scattering and momentum diffusion are weaker for 1 MeV electrons at 45° pitch angles than for 700 keV electrons at 10° pitch angle.

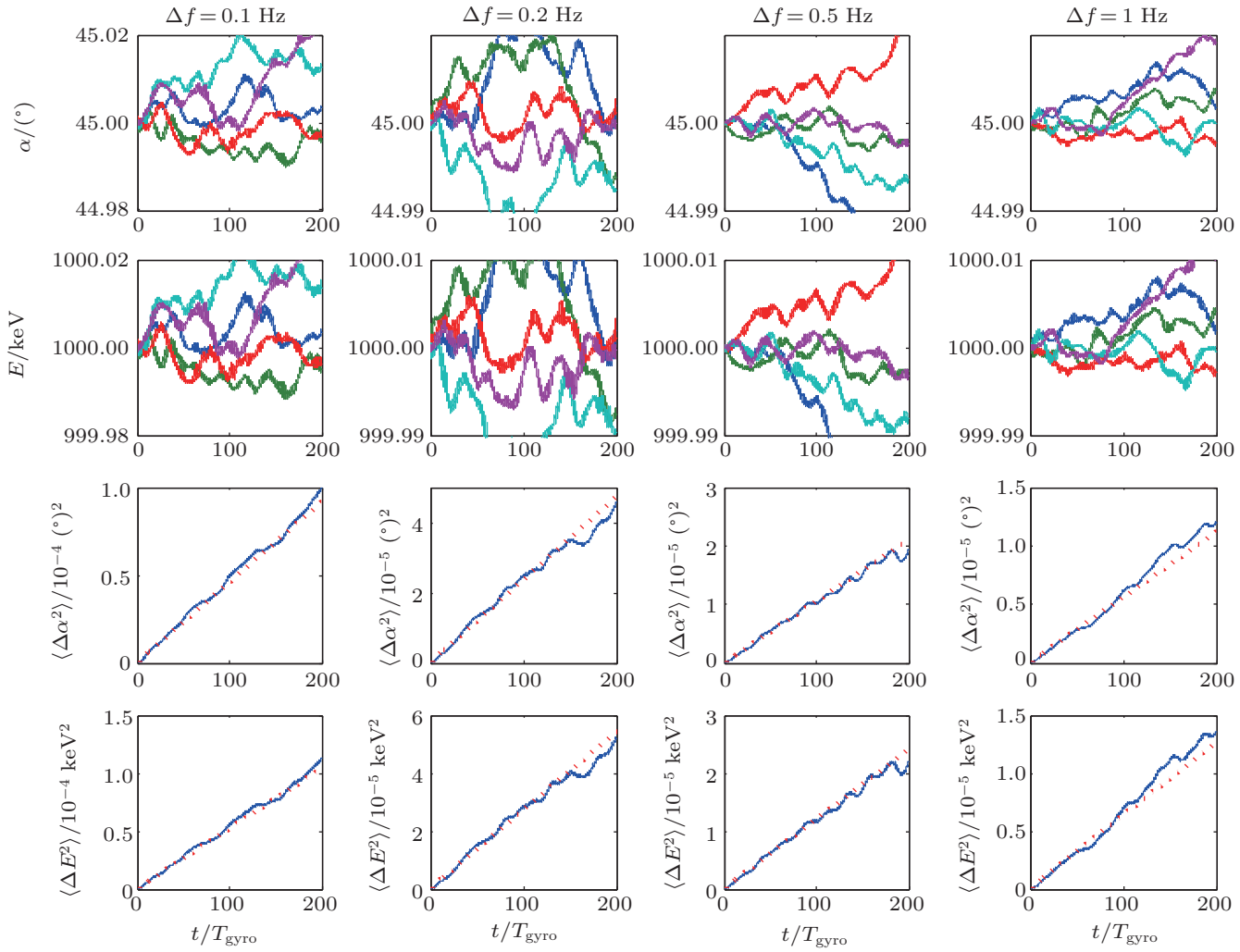


Fig. 4. (color online) The same as Fig. 3 but for 1 MeV electrons with an initial pitch angle of 45°.

To quantitatively evaluate the test particle diffusion rate and investigate its pitch angle dependence, we perform the test particle simulation runs for a number of initial pitch angles for three fixed energies, i.e. 700 keV, 1 MeV, and 2 MeV. According to Fig. 2, the initial pitch angles are chosen to be in a range of 1°–27° in steps of 3° for 700 keV electrons, 37°–48° in steps of 1° for 1 MeV electrons, and 64°–68° in steps of 1° for 2 MeV electrons. Figure 5 shows the curves of momentum diffusion rates versus local pitch angle for the three energies, based on the test particle simulation results. The rates are indicated for four values of the frequency interval Δf, i.e. 0.1, 0.2, 0.5, and 1 Hz.

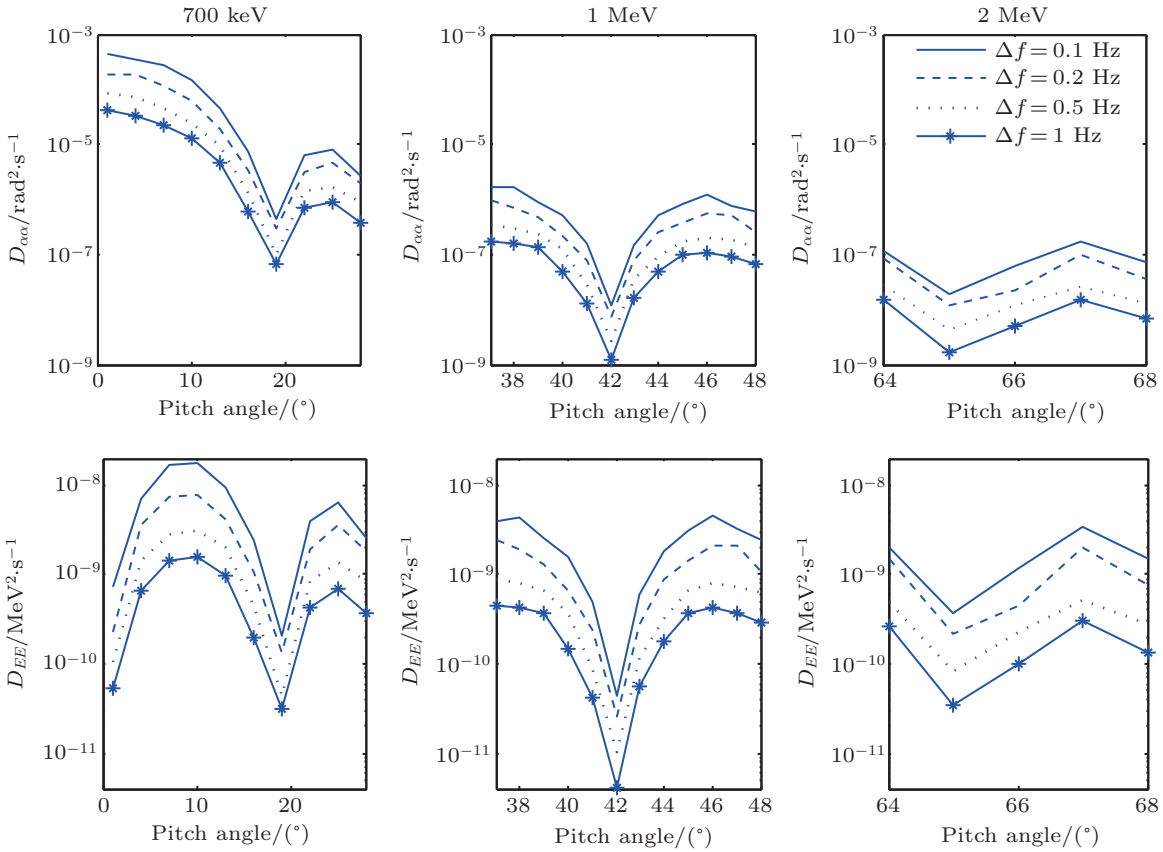


Fig. 5. (color online) Localized pitch angle diffusion rates (top) and momentum diffusion rates (bottom) obtained by test particle simulation for electrons of 700 keV, 1 MeV, and 2 MeV (from left to right) as a function of pitch angle for the four indicated adopted values of the frequency interval Δf.

Regarding the test particle diffusion rates $D^{\rm TP}_{\alpha\alpha}$ and $D^{\rm TP}_{pp}$ as a function of pitch angle, there are a number of important features. (i) Artificially triggered broadband ELF/VLF waves with a nominal amplitude of ~ 1 pT at discrete frequencies can drive intense pitch angle scattering of 700 keV electrons at low pitch angles near the loss cone. In contrast, the induced local diffusion rates of 1 MeV and 2 MeV electrons are much smaller at intermediate and high pitch angles, respectively, suggesting that $D^{\rm TP}_{\alpha\alpha}$ generally decreases with increasing pitch angle and electron energy. (ii) Comparatively, the momentum diffusion ($D^{\rm TP}_{pp}$) driven by artificially generated ELF/VLF waves is minor, mainly due to the high electron density in the plasmasphere. (iii) The test particle diffusion rates show a pronounced dependence on the frequency interval at each pitch angle. The diffusion rates are generally inversely proportional to Δf within the considered range of 0.1 Hz–1 Hz, similar to the results in Figs 3 and 4. (iv) The test particle diffusion rates show non-monotonic variations with pitch angle, which may be attributed to the occurrence of resonances with artificial whistler waves at different frequency components of the 800 Hz–1000 Hz artificial waves.

These features are similar to those for artificial monochromatic (single-frequency) waves.[24] This is to be expected since the resonant scattering effect of broadband waves can be reasonably regarded as a sum of the effects of the frequency components in a narrow band (much narrower than the entire frequency band, 200 Hz). We call such a narrow band the 'effective frequency band', and its central frequency the 'effective central frequency $f_{\rm ec}$'. $f_{\rm ec}$ is different for different pairs of (α, E). For example, $f_{\rm ec}$ is 878 Hz for 700 keV electrons with 10° pitch angle in Fig. 3 and it is 934 Hz for 1 MeV electrons with 45° pitch angle in Fig. 4. For each (α, E), the resonant interaction between electrons and 800 Hz–1000 Hz broadband waves is actually attributed to the interaction with the frequency components in the effective frequency band. More specifically, when Δf increases, the number of frequency com-

ponents in the effective frequency band decreases and thus the number of frequency components that can contribute to electron resonant diffusion decreases to cause slower electron diffusion processes. In this way, we can explain the inversely proportional relationship between test particle diffusion coefficient and frequency interval Δf. However, we speculate that there should be a threshold value of frequency interval above which only one wave frequency lies in the effective frequency band and the resonant scattering effect of broadband waves becomes identical to that of single-frequency waves.

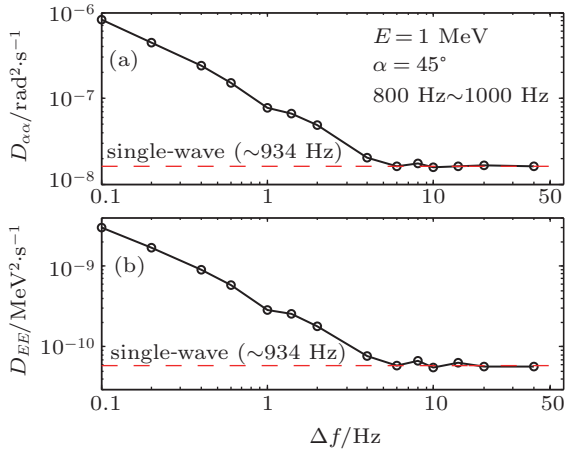


Fig. 6. (color online) Dependences of pitch angle diffusion rate (a) and momentum diffusion rate (b) on frequency interval Δf.

To verify this hypothesis and quantify this threshold value of Δf, we further look into the interactions of 1 MeV electrons at 45° pitch angle with 800 Hz–1000 Hz artificial broadband whistler waves by varying the frequency interval (Δf) value in a much broader range. We reset the frequency components from 800 to 1000 Hz as

$$f_j = f_{\rm m} \pm j\Delta f, \tag{5}$$

where $j = 1, 2, \ldots$, $f_{\rm m} = f_{\rm ec} = 934$ Hz. By doing this, we can make sure that there is at least one effective frequency component in the 800 Hz–1000 Hz range. The values of Δf are arranged to vary from 0.1 Hz to 40 Hz, and the calculated test particle diffusion coefficients as a function of Δf are shown in Fig. 6. Apparently, the diffusion coefficients are inversely proportional to Δf when Δf is below 6 Hz. When Δf is larger than 6 Hz, the diffusion coefficients remain unchanged with increasing Δf, which is consistent with the test particle scattering rates obtained for the interactions of these electrons with the monochromatic waves at 934 Hz (shown as horizontal dashed curves in Fig. 6). Figure 6 confirms the above speculation by illustrating a well defined threshold value of Δf at 6 Hz. It further reveals that modulation frequencies of HF heating of the ionosphere should be selected with intervals less than 6 Hz so that better performance of controlled precipitation of high energy electrons in the plasmasphere by artificial ELF/VLF whistler waves can be achieved.

5. Conclusions and discussion

In the present study we simulate the ray path of ELF/VLF emissions at frequencies in a range of 800 Hz–1000 Hz in the inner magnetosphere on the assumption that these waves are already generated by modulated HF heating of the ionosphere. Following the relativistic resonance condition, we evaluate electron resonant energies of these artificially triggered whistler waves as a function of pitch angle. Finally, the test particle approach is used to investigate the effect of resonant scattering due to these triggered multi-frequency (broadband) ELF/VLF waves and to quantify the wave induced rates of pitch angle scattering and energy diffusion under various frequency intervals. Our major conclusions are summarized as follows.

(I) ELF/VLF waves due to modulated HF heating in the low latitude ionosphere can propagate to higher L shells by magnetospheric reflections, and become highly oblique in the magnetosphere. The wave frequency corresponding to the modulation frequency of the HF carrier strongly affects the spatial extent of the L shell. At the equator of $L = 3$, the artificially triggered ELF/VLF waves at frequencies in a range of 800 Hz–1000 Hz can resonate with electrons with energies ranging from $\sim$ 100 keV to $\sim$ 10 MeV.

(II) Changes in pitch angle and kinetic energy for a set of test electrons due to resonant interactions with discrete, multi-frequency ELF/VLF waves are stochastic. In contrast, the averages of $\Delta\alpha^2$ and ΔE^2 over all test electrons increase monotonically with increasing time and demonstrate a linear tendency, which is similar to that associated with single-frequency waves. Computed local pitch angle diffusion coefficients can be notably efficient at low pitch angles near the loss cone, further supporting the feasibility of the artificial triggering of broadband ELF/VLF whistlers to affect the loss of electrons at energies ranging from several hundred kiloelectronvolts to a few megaelectronvolts in the magnetosphere.

(III) For discrete, multi-frequency waves, there is a threshold value of Δf for which the net diffusion coefficient is inversely proportional to Δf (proportional to the frequency component $N_{\rm w}$) when Δf is below the threshold value, but it remains unchanged with increasing Δf when Δf is larger than the threshold value. This is explained as being due to the fact that the resonant scattering effect of broadband waves is the sum of the effects of each frequency in the 'effective frequency band'. When Δf becomes large, there is only one component in the 'effective frequency band', and the overall diffusion effect of multi-frequency (broadband) waves is nearly equivalent to that of a monochromatic wave. Our results suggest that wave frequencies of artificially generated whistlers can be appropriately selected to have reasonable frequency intervals to seek optimal scattering interactions with high energy electrons in the plasmasphere.

We note that the test particle simulation is performed around the magnetic equator. In other words, it is localized, and thus the background magnetic field, electron density, and wave normal angle are assumed to be constant in each run. Since in the test particle simulation the wave amplitude is set to be constant at each discrete frequency, which is reasonable for artificially generated whistler waves but different from the commonly adopted Gaussian spectrum in the UCLA Full Diffusion Code, we have not yet quantitatively compared our test particle simulation results with the quasi-linear computation results,[6,11,12,35,36] which however will be investigated in detail later. As a matter of fact, as the electrons bounce back and forth along the magnetic field line, bounce-averaging simulations in the inhomogeneous magnetic field geometry, e.g. a dipole field, are more realistic.[37–39] The effects of carrying out bounce-averaging of pitch-angle diffusion coefficients are discussed, for example, by Albert,[40] Summers and Meredith,[10] and Chang *et al.*[24] In general, bounce-averaged diffusion rates are smaller than the local rate. It is also expected that the curve of bounce-averaged scattering rate, plotted as a function of equatorial pitch angle, can become much smoother, as a result of the mixture of the resonant scattering effects at various latitudes with various local pitch angles. Inclusion of the bounce motion and incorporation of test particle simulations in the inhomogeneous magnetic field for electron interactions with artificial whistler waves are left as a subject for our future studies.

Since artificially generated waves are inherently discrete at various single frequencies, here we select broadband waves that are composed of a series of discrete frequencies with a certain frequency interval to represent the artificially generated multi-frequency whistlers due to ionospheric heating. By introducing the term of frequency interval Δf, we find that when Δf is chosen to be above the threshold value, the net diffusion coefficients due to the artificial whistlers do not decrease with increasing Δf, while the total wave power $\sim N_{\rm w}(B_{yj}^{\rm w})^2$ decreases. In this investigation we focus on weak wave components, i.e. 1 pT; therefore, quasi-linear diffusion prevails. More complicated dependence of diffusion effect on total wave power can occur when large amplitude waves are considered and nonlinear effects take place.[41–43] In addition, we note that our present analyses concentrate on localized wave–particle resonant interaction. How the wave–particle interaction process will vary with the adoption of frequency interval Δf in more realistic geomagnetic field morphology will be another subject for our future research.

References

[1] Shprits Y Y, Subbotin D and Ni B B 2009 *J. Geophys. Res.* **114** A11209
[2] Su Z P, Xiao F L, Zheng H N and Wang S 2010 *J. Geophys. Res.* **115** A09208
[3] Su Z P, Xiao F L, Zheng H N and Wang S 2011 *Geophys. Res. Lett.* **38** L06106
[4] Su Z P and Zheng H N 2009 *Chin. Phys. Lett.* **26** 129401
[5] Xiao F L, Su Z P, Zheng H N and Wang S 2010 *J. Geophys. Res.* **115** A05216
[6] Qureshi M N S, Sehar S, Shah H A and Cao J B 2013 *Chin. Phys. B* **22** 035201
[7] Chen Y, Zhao D, Liu W X, Wang Y and Wan X S 2012 *Chin. Phys. B* **21** 104103
[8] Thorne R M 2010 *Geophys. Res. Lett.* **37** L22107
[9] Summers D 2005 *J. Geophys. Res.* **108** A8
[10] Summers D, Ni B B and Meredith N P 2007 *J. Geophys. Res.* **112** A04207
[11] Ni B B, Thorne R M, Shprits Y Y and Bortnik J 2008 *Geophys. Res. Lett.* **35** L11106
[12] Ni B B, Zhao Z Y, Gu X D and Wang F 2008 *Acta Phys. Sin.* **57** 7937 (in Chinese)
[13] Xiao F L, He Z G, Zhang S, Su Z P and Chen L X 2011 *Chin. Phys. Lett.* **28** 39401
[14] Zhang S and Xiao F L 2010 *Chin. Phys. Lett.* **27** 129401
[15] Xiao F L, Chen L, He Y, Su Z P and Zheng H J 2011 *Atmos. Sol-Terr. Phys.* **73** 106
[16] Xiao F L, Yang C, Zhou Q H, He Z, He Y, Zhou X and Tang L 2012 *J. Geophys. Res.* **117** A08204
[17] Xiao F L, Zong Q G, Su Z P, Yang C, He Z G, Wang Y F and Gao Z L 2013 *Sci. Rep.* **3** 1654
[18] Abel B and Thorne R M 1998 *J. Geophys. Res.* **103** 2385
[19] Abel B and Thorne R M 1998 *J. Geophys. Res.* **103** 2397
[20] Inan U S, Chang H C and Helliwell R A 1984 *J. Geophys. Res.* **89** 2891
[21] Inan U S, Bell T F, Bortnik J and Albert J M 2003 *J. Geophys. Res.* **108** 1186
[22] Gu X D, Zhao Z Y, Ni B B, Wang X and Deng F 2008 *Acta Phys. Sin.* **57** 6673 (in Chinese)
[23] Wang P, Wang H Y, Ma Y Q, Li X Q, Lu H, Meng X C, Zhang J L, Wang H, Shi F, Xu Y B, Yu X X, Zhao X Y and Wu F 2010 *Acta Phys. Sin.* **60** 039401 (in Chinese)
[24] Chang S S, Ni B B, Zhao Z Y, Wang F, Li J X, Zhao J J, Gu X D and Zhou C 2014 *Acta Phys. Sin.* **63** (in Chinese)
[25] Barr R and P Stubbe 1991 *Geophys. Res. Lett.* **18** 1035
[26] Platino M, Inan U S, Bell T F, Parrot M and Kennedy E J 2006 *Geophys. Res. Lett.* **33** L16101
[27] Piddyachiy D, Inan U S, Bell T F, Lehtinen N G and Parrot M 2008 *J. Geophys. Res.* **113** A10308
[28] Ferraro A J, Lee H S, Allshouse R, Carroll K, Tomko A A, Kelly F J and Joiner R G 1982 *J. Atmos. Terr. Phys.* **44** 1113
[29] Bortnik J 2005 "Precipitation of Radiation Belt Electrons by Lightning-Generated Magnetospherically Reflecting Whistler Waves", (Ph. D. dissertation) (California: Stanford University)
[30] Wang F, Zhao Z Y, Chang S S, Ni B B and Gu X D 2012 *Acta Phys. Sin.* **61** 199401 (in Chinese)
[31] Shklyar D R, Parrot M, Chum J, Santolik O and Titova E E 2010 *J. Geophys. Res.* **115** A05203
[32] Tao X, Bortnik J, Albert M J, Liu K and Thorne R M 2011 *Geophys. Res. Lett.* **38** L06105
[33] Bortnik J and Thorne R M 2010 *J. Geophys. Res.* **115** A07213
[34] Tao X and Bortnik J 2010 *Nonlinear Processes Geophys.* **17** 599
[35] Xiao F L, Zong Q G and Chen L X 2009 *J. Geophys. Res.* **114** A01215
[36] Xiao F L, Su Z P, Zheng H N, and Wang S 2009 *J. Geophys. Res.* **114** A03201
[37] Su Z P, Zhu H, Xiao F L, Zheng H N, Shen C, Wang Y and Wang S 2012 *J. Geophys. Res.* **117** A09222
[38] Su Z P, Zhu H, Xiao F L, Zheng H N, Shen C, Wang Y and Wang S 2013 *J. Geophys. Res.* **8** 1
[39] Zhu H, Su Z P, Xiao F L, Zheng H N, Shen C, Wang Y and Wang S 2012 *J. Geophys. Res.* **117** A12217
[40] Albert M J 1999 *J. Geophys. Res.* **104** A22429
[41] Jiang H, Yang X X, Lin M M, Shi Y R and Duan W S 2011 *Chin. Phys. B* **20** 019401
[42] Zahedian M, Maraghechi B and Rouhani M H 2012 *Chin. Phys. B* **21** 034101
[43] Tao X, Bortnik J, Albert M J, Thorne R M and W Li 2013 *J. Atmos. Terr. Phys.* **99** 62